Chapter 3

Light in the Polar Night

Jonathan H. Cohen, Jørgen Berge, Mark A. Moline, Geir Johnsen and Artur P. Zolich

Abstract

How much light is available for biological processes during Polar Night? This question appears simple enough. But the reality is that conventional light sensors for measuring visible light (~350 to ~700 nm) have not been sensitive enough to answer it. Beyond this technical challenge, "light" is a general term that must be qualified in terms of "light climate" before it has meaning for biological systems. In this chapter, we provide an answer to the question posed above, and explore aspects of light climate during Polar Night with relevance to biology. Specifically, how Polar Night is defined by solar elevation; atmospheric light in Polar Night and its propagation underwater; bioluminescence in Polar Night and the concept of Polar Night as a deep-sea analogue; light pollution; and future perspectives. This chapter focuses on the quantity and quality of light present during Polar Night, while subsequent chapters in this volume focus on specific biological effects of this light for algae (Chapter 4), zooplankton (Chapters 5, 8), and fish (Chapter 7).

Jonathan H. Cohen
School of Marine Science and Policy
University of Delaware
700 Pilottown Road
Lewes, DE 19958 USA
jhcohen@udel.edu

Jørgen Berge
UiT The Arctic University of Norway
Department for Arctic and Marine Biology
N-9037 Tromsø, Norway
Jorgen.berge@uit.no

Mark A. Moline
School of Marine Science and Policy
University of Delaware
700 Pilottown Road
Lewes, DE 19958 USA
mmoline@udel.edu

Geir Johnsen
Centre of Autonomous Marine Operations and Systems (AMOS),
Department of biology, Norwegian University of Technology and Science (NTNU)
N-7491 Trondheim, Norway
Geir.johnsen@ntnu.no

Artur P. Zolich
Centre of Autonomous Marine Operations and Systems (AMOS),

Department of engineering cybernetics, Norwegian University of Technology and Science (NTNU)
N-7491 Trondheim, Norway
Artur.zolich@ntnu.no

3.1 What is Light Climate?

There are several excellent reviews on light and its biological relevance in general (Land and Nilsson 2012; Johnsen 2012; Cronin et al. 2014), and in the polar environment specifically (Sakshaug et al. 2009; Pavlov et al. 2019), and we refer you to these for further details on physical aspects of light, and how organisms detect and use it. Here, we highlight the concept of light climate, as it includes the key elements needed to understand light during Polar Night.
Specifically, light climate comprises the *intensity*, *spectrum*, and *duration* of light for a given location. Each of these parameters can be considered in a variety of units, and crucially for their biological relevance, each are species-dependent (see Box 3.1). We briefly discuss some fundamental considerations for each parameter concerning measurement and units.

3.1.1 Intensity

Light intensity can be measured as radiance (L) or irradiance (E) (Fig. 3.1A). Radiance refers to photons emitted per unit area per second, while irradiance refers to photons received per unit area. The angle of the sensor is variable for either quantity, but typically in biological studies directional measurements concern downwelling light (L_d, E_d) or upwelling light (L_u, E_u). Irradiance is typically measured in "hemispheres" where the collector may either be cosine-weighted to favor photons normal to the collector face (cosine), or equally capture photons from all angles of the 180° hemisphere (2π). Alternatively, scalar irradiance (E_o) measurements can be made with a 4π collector which encompass both downwelling and upwelling light over 360°, mimicking the absorption surface of an algal cell in the water column. Irradiance is commonly measured in energy units (W m^{-2}) or quantal units (photons s^{-1} m^{-2} or µmol photons s^{-1} m^{-2}), with the latter particularly useful for studies of photosynthesis and vision. A common confusion concerning intensity measurements involves photometry versus radiometry. Radiometry concerns measurements of radiance and irradiance. Photometry concerns measurements of luminance and illuminance, which are analogous, but involve weighting the measurement by photopic human visual sensitivity and are expressed in terms of lumens. Photometric measurements are not directly relevant to biological processes apart from human vision.

3.1.2 Spectrum

No matter how intensity is measured, the spectral composition of the ambient light and the spectral window of the sensor must be considered (Fig. 3.1B). One way to do this is to measure both intensity and spectrum simultaneously with a hyperspectral light sensor, providing measurements of L, E, and E_o per nanometer across the spectral window of the sensor. However, a common approach to light measurement in biological studies is to report a value for "Photosynthetically Active Radiation" or PAR, which is light intensity integrated from 400-700 nm. While this light range encompasses wavelengths responsible for many biological processes (e.g., photosynthesis, vision, entrainment of endogenous rhythms), it must be remembered that "PAR" only denotes the spectral range of the measurements, so radiance or irradiance as described above could both be measured as PAR. For an irradiance measurement, clearly defining a measurement as, for example, $E_{o,PAR}$, resolves this issue.

3.1.3 Duration

The diel (24h) cycle of light can be considered in terms of its photoperiod (Fig. 3.1C). In this way, the light portion of the 24h cycle is denoted as “day” or “photophase”, and the dark portion as “night” or “scotophase”. Photoperiod then is expressed as [hours day]:[hours dark]. For some biological processes, such as photosynthesis, day represents the active period (i.e., actinic light providing photosynthesis) while night represents the inactive period (see Chapter 4). However, the active phase may occur at night for other processes, such as nocturnal diel vertical migration (Chapter 5). Photoperiod can entrain biological clocks, providing information on time of year needed to control patterns of physiology and behavior (Chapter 8). An open question concerning measurement of photoperiod is what light level to consider as the break between “day” and “night”. This will ultimately depend on the light sensing ability of the organism in question (see Box 3.1 and section 3.7 below).

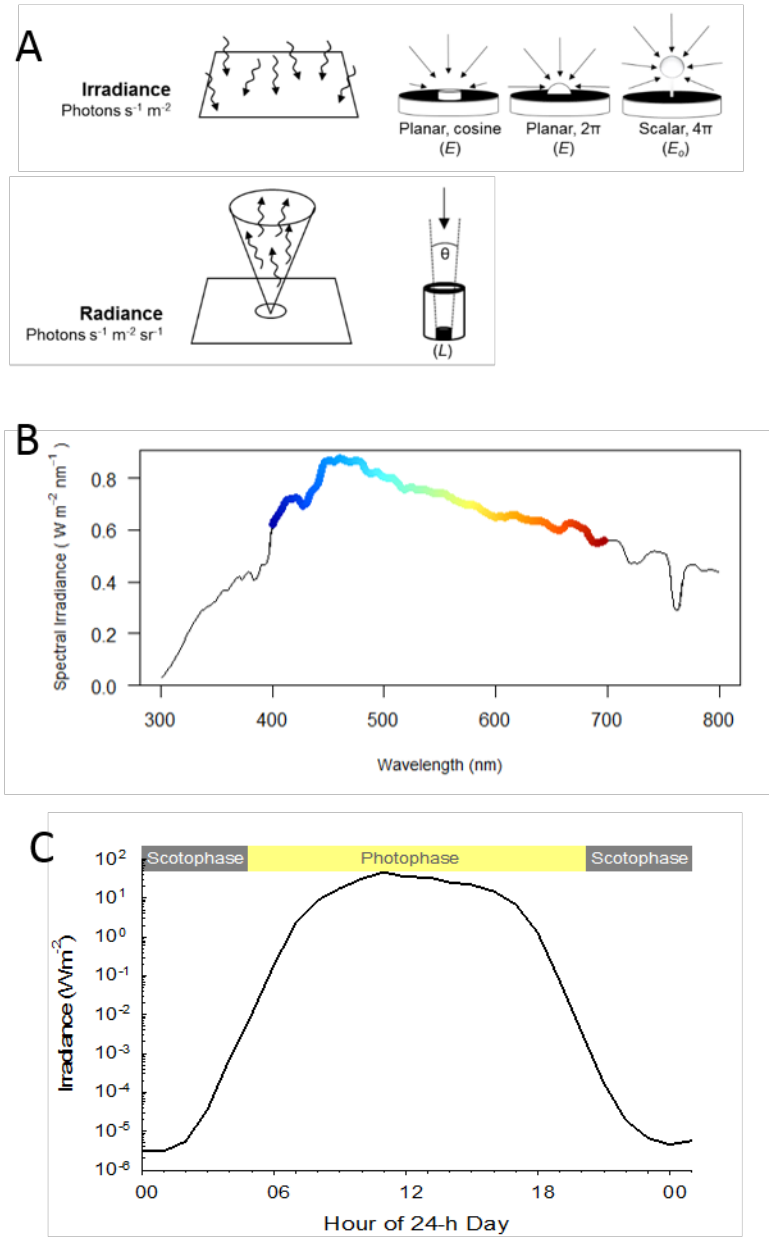

Fig 3.1 Measurement considerations for light climate. (**a**) Irradiance and radiance provide different, yet complementary ways to quantify environmental light. (**b**) Spectral irradiance at Ny-Ålesund, replotted from Hisdal (1986). These are global radiation values (direct solar radiation and diffuse radiation from reflected/scattered sunlight). Colored points indicated the spectral range for Photosynthetically Active Radiation (PAR, 400-700 nm), with colors at these wavelength as they appear to the human visual system. Note that spectral irradiance is not flat over this region, and there is incident light outside of the PAR region. (**c**) An example of photoperiod where irradiance changes over the 24-h day. Periods of scotophase (night) and photophase (day) are indicated. The duration of these periods is variable, depending on e.g. location and light source

Box 3.1 Biological utilization of light in polar night

According to the First Law of Photochemistry (Albini 2016), light must be absorbed for photochemistry to occur. This implies that if the photochemical capacity for absorbing light of a particular wavelength is not present in an organism, then photobiology (e.g., photosynthesis, vision, light-directed movement, etc.) will not take place, irrespective of the intensity or duration of exposure. It is critical then to consider the spectral absorbance of the molecules responsible for absorbing light and initiating downstream biological processes, and what the resulting spectral sensitivities might mean for light-mediated biology during polar night (Chapters 4-8).

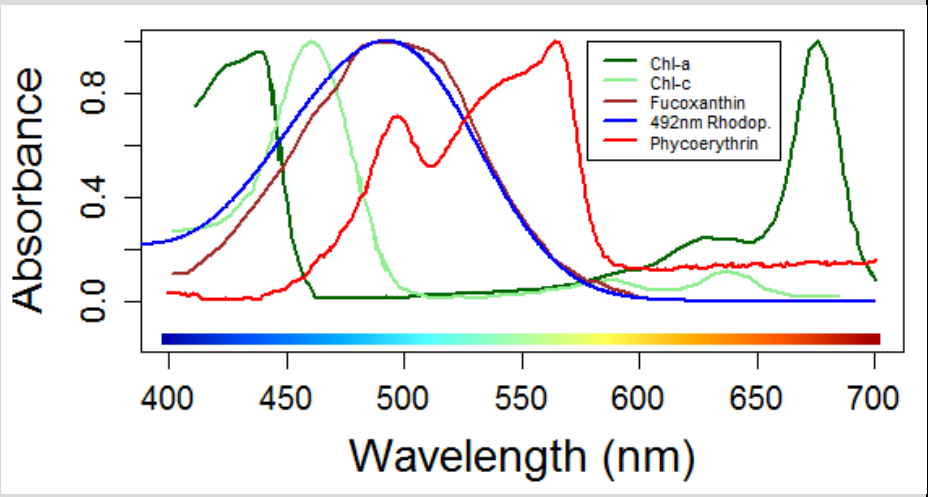

Ice algae, planktonic algae, and benthic macroalgae possess a wide range of light-absorbing pigments (see Chapter 4), which can include chlorophylls absorbing in the blue (400-500nm) and red (600-700nm) regions, carotenoids (e.g., fucoxanthin) absorbing mostly at 400-530 nm and phycobiliproteins (e.g., phycoerythrin) as example) with high absorption in the green-orange region (500-570nm). Collectively, these pigments provide broad spectral coverage, but information in specific spectral channels may be used by the organism in different ways. For example, high energy blue light can selectively upregulate genes responsible for photoprotection, while lower energy red light selectively affects photosynthetic efficiency (Valle et al. 2014). However, there does not appear to be enough light at necessary wavelengths during polar night to allow for algal photosynthesis (Chapter 4).

Animals, including planktonic and benthic invertebrates and fish, possess both visual and non-visual light-sensitive pigments. Among marine animals, rhodopsin is the visual pigment, which contains a chromophore *retinal* derived from vitamin-A1, and a protein moiety *opsin* which determines the spectral sensitivity of the pigment. Some species have a single rhodopsin spectral class and thus a relatively narrow spectral sensitivity (e.g., krill with a 492nm Rhodop.; Cohen et al. 2015), while other species have multiple spectral classes and a broader spectral sensitivity (e.g., Atlantic cod with 490 and 550 nm Rhodop.; Anthony and Hawkins 1983). Marine animal visual systems (and likely their non-visual light-sensing pigments as well) have sufficient sensitivity for light-mediated processes during polar night (copepods, Båtnes et al. 2013; krill, Cohen et al. 2015; scallops, Tran et al. 2016; fish, Vollset et al. 2011) (Chapters 5, 7, 8). Scattering layers of zooplankton and fish clearly exhibit diel vertical migration (Ludvigsen et al. 2018) and lunar vertical migration during polar night (Last et al. 2016). The extent to which spectral cues resulting from solar and lunar elevation (e.g., Chappuis Effect) may be involved in DVM and LVM (Chapter 5), or in seasonal timekeeping (Chapter 8), remain unknown.

3.2 Polar Night as defined by solar elevation

In its most simple definition, ***Polar Night*** (or *perpetual night*; The Norwegian Arctic Pilot, 2018) occurs when the sun remains below the horizon throughout a full diel cycle. That is, solar elevation remains less than 0° over the 24-h day. When considering the number of days each year that this occurs, the duration of Polar Night increases by approximately 6 days for each degree of latitude (Fig 3.2A). Thus, Polar Night lasts ~1 month at 68° N, 3.5 months at 78° N, and 5.5 months at 88° N, extending to a full 6 months at the North Pole. At the southern hemisphere, the Polar Night can be defined in exactly the same terms. However, with a focus on the marine system, the two hemispheres are "poles apart" in more than one respect – while the marine Arctic cover nearly the entire region north of 80°N, the Southern Ocean does not go beyond 80°S. Hence, we will in this chapter not focus on the Antarctic and Southern Ocean, although all definitions, parameters and processes that are defined by the sun's elevation relative to the horizon are also valid for the Southern Hemisphere.

As introduced in Chapter 1, the above definition assumes that Polar Night is a static event. However, the Polar Night is anything but static. Rather, it can better be thought of as an annual process with four different levels of light (Polar twilight, Civil Polar Night, Nautical Polar Night, and Astronomical Polar Night), with each level defined by the sun's elevation relative to the horizon. Hence, the exact level of Polar Night at any given location depends not only on latitude (Fig 1.5), but also have a temporal component. While these definitions adequately describe Polar Night in an annual context, solar elevation is constantly changing over the diel cycle, whether the sun is visible or not. So understanding light climate during any of the four levels of Polar Night also requires further consideration of solar elevation in terms of the gradation of ***twilight***. Twilight is defined based on the sun's elevation below the horizon at any moment (Fig 3.2B). **Civil twilight** occurs when solar elevations are between the horizon and 6° below it. **Nautical twilight** occurs when solar elevations are 6° to 12° below the horizon. **Astronomical twilight** occurs when solar elevations are 12° to 18° below the horizon. Beyond this is "darkness" (Table 3.1). These definitions are useful for understanding light during Polar Night in two ways. First, at any point in the diel (24 h) cycle during Polar Night, the gradation of twilight can be identified, which then provides a measure of light intensity at that time (Fig 3.2B). Second, any given day during Polar Night can be categorized according to the level of twilight occurring at solar noon. This provides a useful way to think about Polar Night at a given latitude.

Table 3.1 Definitions of Polar Night and twilight based on solar elevation. Polar Night definitions are for solar elevation at the winter solstice, while for twilight the definitions apply at any point in the solar day (see Urban and Seidelmann, 2013). Note that "darkness" does not necessarily mean the total absence of light. Relevant latit2udes are based on geometric positions of the sun (see Chapter 1 for further details). Note that the notations of twilight and Polar Night are different.

Solar Elevation (°)	**Polar Night Definition**	**Twilight Definition**	**Relevant latitude (N and S) at noon on winter solstice**
0 to -6	polar twilight	civil twilight	66-72°
-6 to -12	civil polar night	nautical twilight	72-78°
-12 to -18	nautical polar night	astronomical twilight	78-84°
less than -18	astronomical polar night	darkness	84-90°

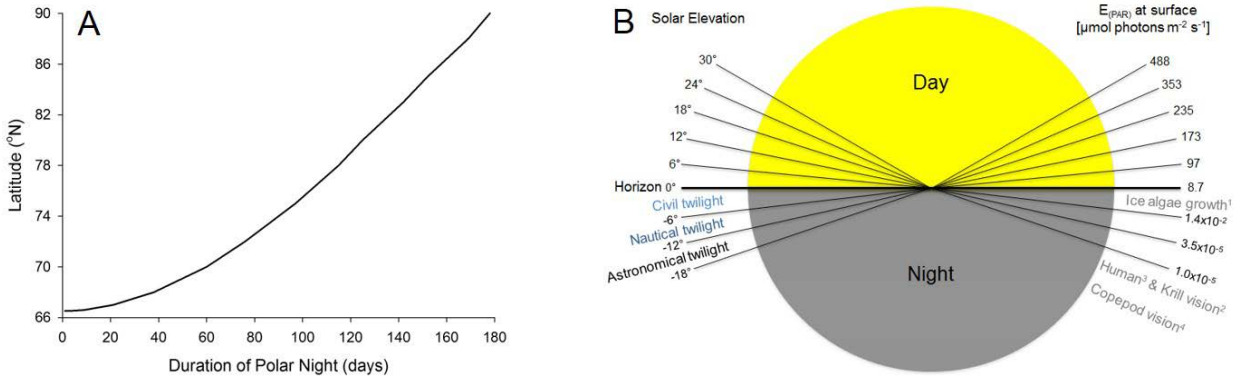

Fig 3.2 Polar light environment with respect to solar elevation. (**a**) Duration of Polar Night as a function of latitude, where Polar Night is defined as the sun remaining below the horizon throughout the 24-hour day. These durations are based on apparent solar elevation (see Chapter 1). (**b**) Gradations of twilight. Solar elevations (left labels) are shown with corresponding atmospheric light intensities (right labels) taken as the median measured E_{PAR} (400-700nm, Photosynthetically Active Radiation) for a given solar elevation (± 1°) measured at the light observatory, Ny-Ålesund, Svalbard. Solar elevations corresponding to Civil twilight (-0° to -6°), Nautical twilight (-6° to -12°), and Atmospheric twilight (-12° to -18°) are indicated on the left scale, while irradiance thresholds for select biological processes are indicated on the right scale. [1]Hancke et al. 2018; [2]Myslinski & Frank 2005; [3]Rieke & Baylor 1998; [4]Båtnes et al. 2013

3.3 Atmospheric light in the Polar Night

The seasonal cycle of sunlight drives annual patterns in polar ecosystems, most notably primary productivity (Chapter 4). While a characteristic lack of the sun above the horizon defines Polar Night, it does not mean that light from the sun is completely absent from the sky at this time of year. Rather, diffuse light from the sun below the horizon is a distinctive part of the light field during Polar Night, as it is at lower latitudes during twilight. Moonlight, which is reflected sunlight, likewise can play an important biological role during Polar Night. In fact, during periods characterized by nautical or astronomical twilight, lunar illumination during the full moon becomes the dominant ambient illuminator. In addition, the solar winds causing atmospheric molecules to emit light as the aurora borealis (northern lights) will also be a contributor to the ambient light during Polar Night. Therefore, the orb of the sun itself may not be an obvious feature of the Polar Night sky at first glance, but the sun plays a major role in the atmospheric light field of the Polar Night. Beyond the sun, starlight represents another light source of potential relevance during Polar Night. Each of these light sources has a characteristic intensity and spectrum, which we explore below, as well as photoperiod (see section 3.7).

3.3.1 Intensity

Arguably, the most complete record of the annual light intensity cycle in the Arctic comes from observations made at Ny-Ålesund, Svalbard (78.9° N, 11.9° E). Since 1992, the Alfred Wegener Institute for Polar and Marine Research (AWI) has made surface radiation measurements (pyrheliometer, pyranometer, pyrgeometer) through the Baseline Surface Radiation Network (BSRN) (Maturilli et al. 2015). At this location, Polar Night occurs 24 October - 18 February, while Polar Day (i.e., Midnight Sun) occurs 18 April - 24 August, with direct sunlight reaching

Ny-Ålesund 8 March - 8 October given the surrounding mountains. The Ny-Ålesund BSRN data are extremely valuable for satellite observations and climate models, but the sensor suite lacks instruments optimized for light measurements relevant to biology. The most relevant detector in this time series is a pyranometer for diffuse shortwave radiation (200 - 3,600 nm), which is too spectrally broad in its sensitivity to relate to biological processes. For example, PAR is used as a proxy for biologically available light (e.g. photosynthesis and vision), and these are only a fraction of the wavelengths contributing to the diffuse shortwave radiation measurement (e.g., Fig. 3.1B). Additionally, the BSRN shortwave pyranometer is only sensitive enough to detect light during sunlit portions of the year (February-October), so no data from the Ny-Ålesund BSRN pyranometer are available for Polar Night.

To address this gap, a light observatory was established in January 2017 at the new Geodesy station at Brandalspynten, Kongsfjorden (Zolich 2018) 4km away from the settlement itself. This location was chosen to provide infrastructure and access, while minimizing light pollution from the settlement at Ny Ålesund. This light observatory (*ArcLight*) was put into operation providing data with high (1 hour) temporal resolution throughout the year, including during Polar Night. It is located in heated hut with a transparent plexiglas dome on the roof providing a 180° view towards the atmosphere. The *ArcLight* observatory consists of three sensors (Fig 3.3): (1) a spectroradiometer provides cosine-corrected downwelling spectral irradiance ($E_{d\lambda}$) at 1 nm spectral resolution from 350-800 nm; (2) a digital camera (full size sensor) with an 8 mm lens providing a 180° "fish eye" view of the sky (mimicking a planar cosine corrected irradiance light collector; Fig. 3.1A), and calibrated to deliver irradiance in red, green and blue channels; and (3) a custom irradiance sensor provides a high dynamic sensitivity range from bright summer to dark winter values. All sensors are remotely controlled, acquiring data at user specified intervals. The spectroradiometer and camera are calibrated for units of energy [W m^{-2} nm^{-1}] or quanta [µmol photons m^{-2} s^{-1} nm^{-1}]. The suite of sensors provides sufficient data to extract a range of light regime parameters, including spectral irradiance (E_{λ}), irradiance in the visible spectral range (E_{PAR}), irradiance in RGB channels (600-700nm, 500-600nm, 400-500nm, respectively), day length, cloud cover, light pollution, sun phase, moon phase, northern light dynamics, starlight, rain and snow conditions.

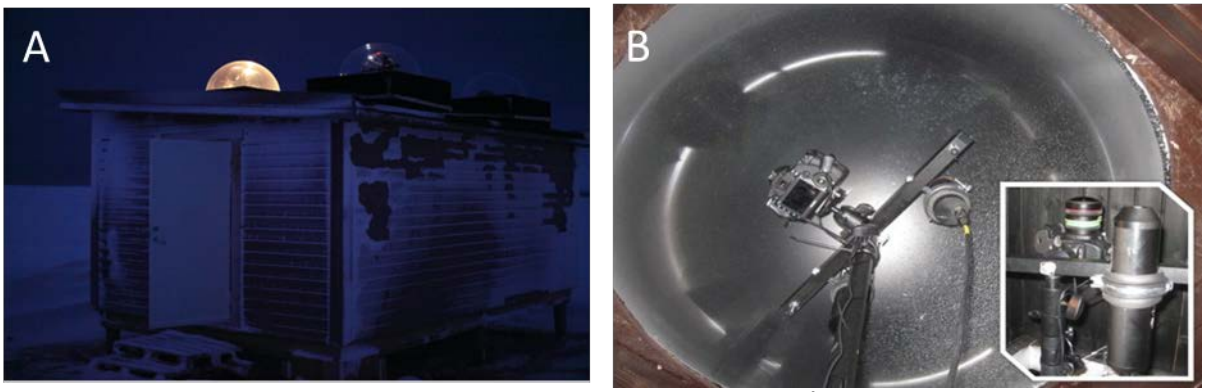

Fig 3.3 ***ArcLight*** **Observatory and sensors outside Ny-Ålesund**. (**a**) ArcLight observatory during Polar Night, with dome illuminated during service of sensors. (**b**) InSitu Marine Optics Ussimo spectroradiometer and Cannon 5D Mark III digital camera with fish eye lens pointing upwards through the plexiglass dome. Inset shows the spectroradiometer and camera laterally. Photos: Geir Johnsen

Not only is the annual cycle of light intensity into and out of the midnight sun resolved in *ArcLight* observatory camera-based measurements (Fig 3.2, 3.4A), but biologically relevant irradiance throughout Polar Night is reliably measured and quantified (Fig 3.4B). This effectively covers a seasonal quantal range of 8-9 orders of magnitude (Zolich 2018, Pavlov et al. 2019). From these data measured at sea level at 79° N, maximum E_{PAR} around 1200 μmol photons m^{-2} s^{-1} is typically found during mid-summer in June at solar noon. In contrast, the maximum E_{PAR} at solar noon (brightest time of day) during the darkest part of Polar Night at this latitude (nautical Polar Night, astronomical twilight) ranged between 1–1.5 x 10^{-5} μmol photons m^{-2} s^{-1} in clear weather conditions and with the moon below the horizon. Hence, values reflect not only diffuse solar illumination, but also potentially light pollution from Ny-Ålesund. Cohen et al. (2015) likewise reported E_{PAR} at solar noon in Ny-Ålesund during mid-January to be ~1x10^{-5} μmol photons m^{-2} s^{-1}, which is consistent with the *ArcLight* time series. Measurements reported in Cohen et al. (2015) were made with the moon below the horizon, whereas the *ArcLight* time series provides the opportunity to see irradiance changes over the lunar cycle. Indeed, the full moon is a striking feature during Polar Night, and its 29-day period is evident in this light record. E_{PAR} is ~100-fold higher during the full moon as compared to the new moon period (Fig 3.4B,C; Fig 3.5B,C). Thus, the full moon increases light intensity during astronomical twilight to levels occurring between civil and nautical twilight. This is consistent with measurements made during dusk at 36° N by Palmer and Johnsen (2015) who reported moonlight affecting downwelling irradiance when solar elevations exceeded -8°. It is important to note that during the new moon, any "ambient" irradiance recorded at this location could include (1) diffuse light from the sun, (2) a range of other natural atmospheric sources (integrated starlight, zodiacal light, airglow and aurora; see Johnsen 2012, Cronin et al. 2014), and (3) light pollution from Ny-Ålesund. Indeed, Ludvigsen et al. (2018) reported diffuse skylight irradiance (350-730nm) as low as 10^{-8} μmol photons m^{-2} s^{-1} in Kongfjorden away from Ny-Ålesund, but these measurements were likely influenced by occlusion of the sky by surrounding mountains. Further work is needed to determine ambient light values during Polar Night absent of light pollution.

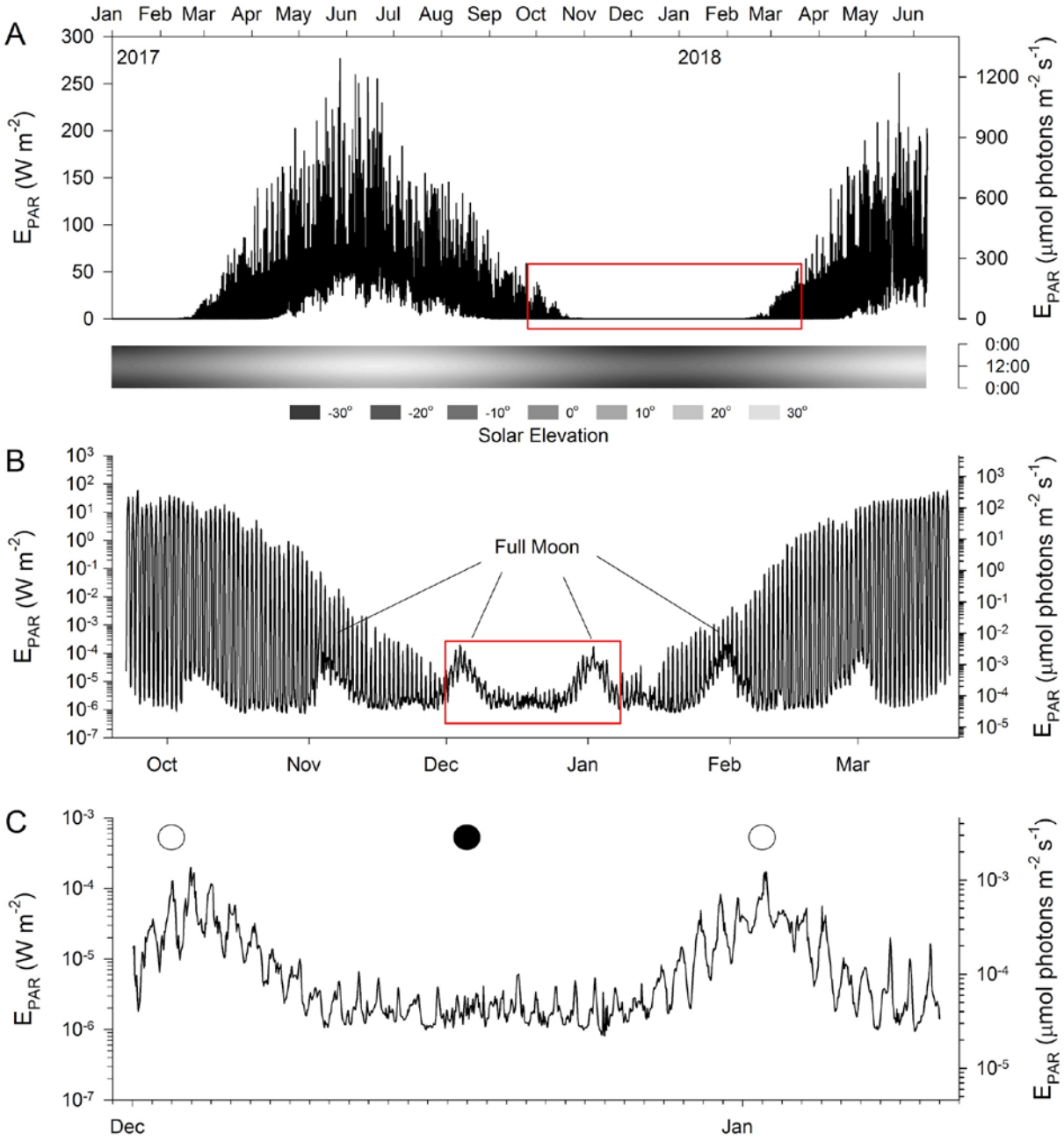

Fig 3.4 Atmospheric irradiance (E_{PAR} recorded at the *ArcLight* Observatory 4 km away from Ny-Ålesund. (**a**) Annual cycle of E_{PAR} from January 2017 - June 2018. Corresponding solar elevation across the 24-h day is plotted below the panel. (**b**) Light data for the Polar Night period falling between the autumn and spring equinox (red box in panel A). (**c**) Light data for December 1, 2017 - January 11, 2018 and centered on the winter solstice (December 21). Open and closed circles show the days of the full and new moons, respectively. E_{PAR} measured during the new moon represents darkest "ambient" light lowest annual polar night irradiance) at Ny-Ålesund, which likely includes both natural and anthropogenic sources. Data are re-plotted from Zolich (2018)

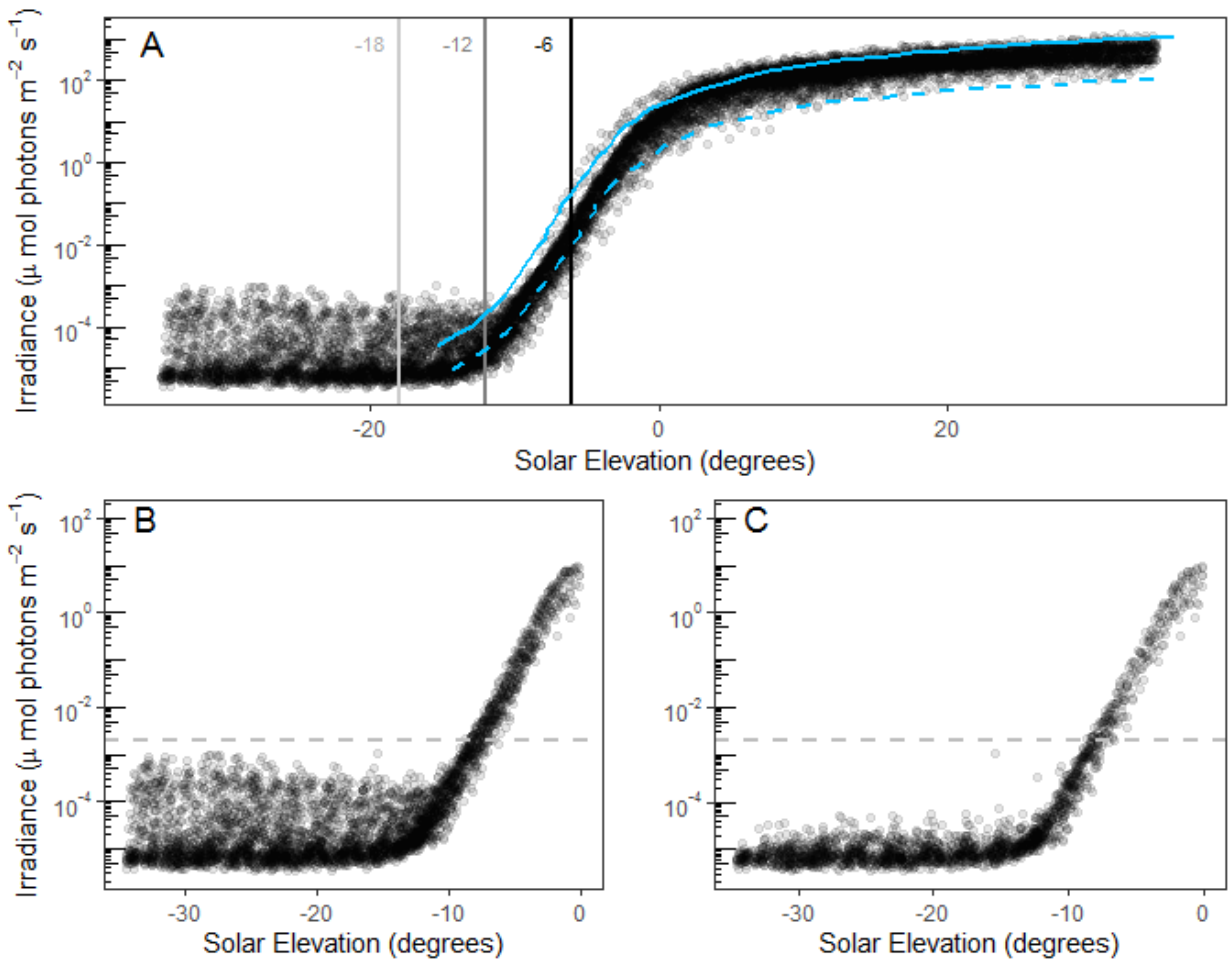

Fig 3.5 Variation in atmospheric light with changes in solar elevation and lunar stage. (**a**) Light data from Fig 3 are plotted here as a function of solar elevation. Vertical lines at -18°, -12°, and -6° indicate lower limits of atmospheric, nautical, and civil twilight. Blue lines are based on data from Bond and Henderson (1963) for clear sky (solid line) and overcast sky (dashed line), converted from illuminance using a conversion factor of 0.0185. (**b**) Light data for only Polar Night (days with elevation at solar noon <0°). The dashed horizontal line denotes irradiance of a full moon at 32° elevation (from Bond and Henderson (1963)), corresponding to the maximum lunar elevation during this time series. (**c**) Data as for panel B, except only for days where the lunar disk was <50% full

3.3.2 Spectrum

The spectral (wavelength) composition of light is fundamental to its biological impact. For sunlight, its spectral composition is dependent on solar elevation. Solar elevations at midday during Polar Night are comparable to twilight periods occurring during dawn and dusk at lower latitudes (Fig. 3.2 and Table 3.1). This means that the spectral composition of diffuse skylight during Polar Night is quite similar to the spectral composition during dawn/dusk periods at lower latitudes. For the sun at elevations just below the horizon during civil twilight (0 to -6°), this involves an increase at blue wavelengths transitioning to a combination of blue and red (Figs. 3.6, 3.7B). This appears magenta to the human eye, and results from a reduction at yellow wavelengths selectively absorbed by atmospheric ozone as the path-length of solar light through the atmosphere increases during nautical twilight (-6 to -12°), a phenomenon termed the *Chappuis Effect*. Skylight then reddens during astronomical twilight (-12 to -18°) due to airglow and integrated starlight (see Johnsen 2012 for details).

These characteristic shifts in the spectral composition of skylight with solar elevation can be further influenced by the presence of the moon (Palmer and Johnsen 2015). Moonlight is reflected sunlight, thus when either of these celestial objects is well above the horizon their spectral compositions are similar, with a peak at blue wavelengths gradually reducing through red wavelengths (Fig. 3.7). Accordingly, the general effect of moonlight on skylight spectral composition during Polar Night will be to increase longer-wavelength visible light (yellows and reds). This is evident in a 24-h spectral time series from Ny-Ålesund (Fig. 3.6), where the increase in E_λ at solar noon shows a characteristic “twilight” spectrum with blue and red peaks which then transitions into a blue-dominated spectrum as the lunar elevation increases well-above the horizon. This is also evident when comparing normalized spectral composition of skylight for early May (sun above the horizon, moon below; Fig. 3.7A) and early February (moon above the horizon, sun below; Fig. 3.7B) at Ny-Ålesund. When the sun is above the horizon and its elevation decreases to minimum around midnight (May), loss of yellow wavelengths is observed at that point. However, when the moon is above the horizon and its elevation increases to a maximum around midnight, a gain of yellow wavelengths is apparent.

Ultimately, the elevation of the sun and moon is critical to the spectral composition of the light produced at any given point during the 24-h day. Above this background “solar” spectrum, however, aurora provides a distinct light feature during Polar Night (Fig. 3.6). This light is spectrally narrow, with portions at several discrete wavelengths (e.g., 391 nm, 557 nm, and 630 nm). Accordingly, while aurora is clearly distinguished above solar/lunar light at these wavelengths, its overall contribution to biologically relevant light appears limited.

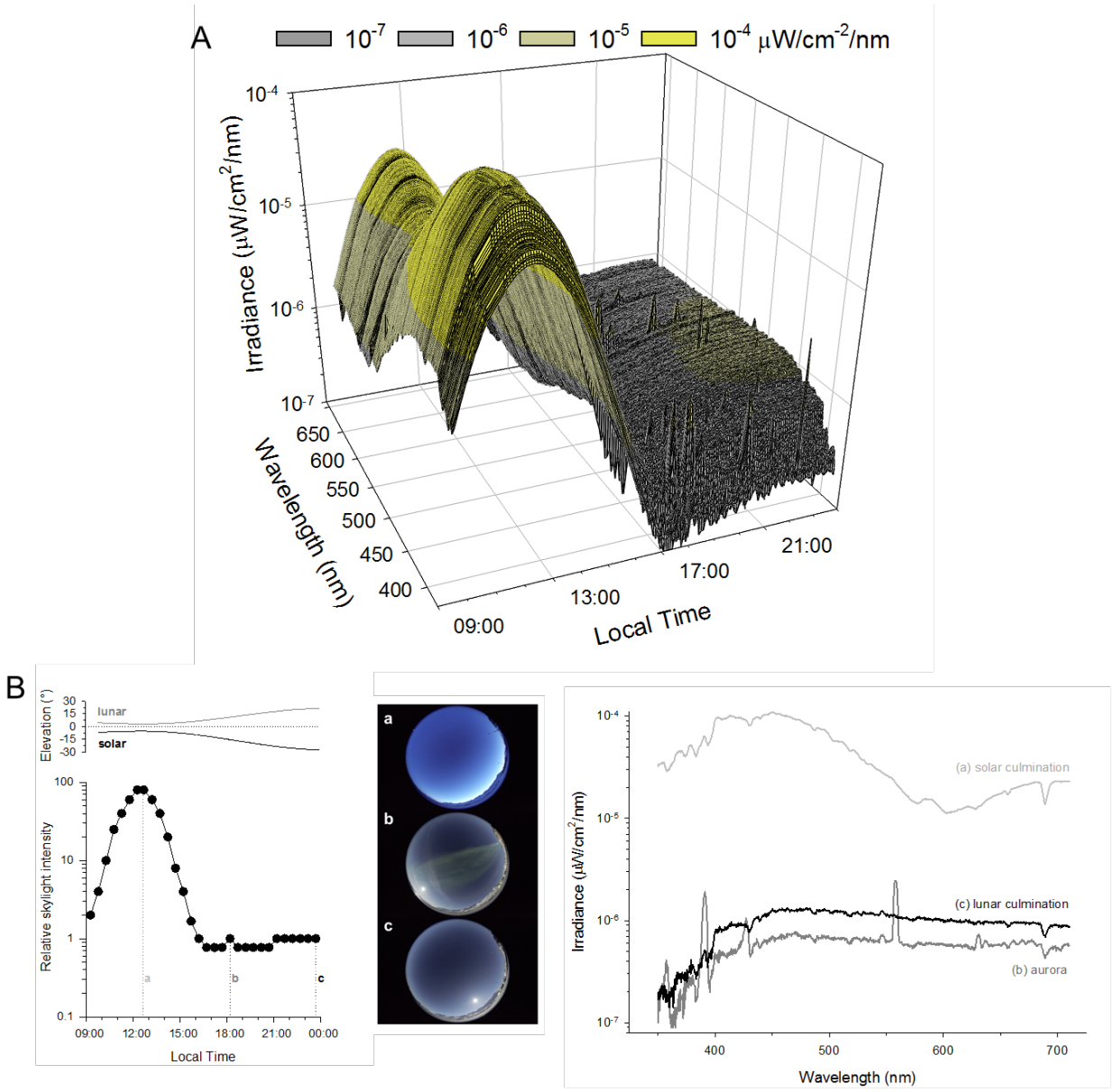

Fig 3.6 Spectral composition of the diel atmospheric light cycle at Ny-Ålesund during Polar Night. (**a**, upper panel) Spectroradiometric measurements of diffuse skylight irradiance at 5 min intervals (see Cohen et al. 2015 for collection details) show a distinct spectral composition as the nears the horizon (blue and red wavelengths dominate with loss of yellows) which then changes to a flatter spectrum as solar elevation becomes more negative and moonlight dominates. At culmination (i.e., maximum elevation), solar and lunar elevations were -6° and 25.2° respectively. (**b**, two lower panels) All-sky camera images were taken at 30 min intervals coincident with the spectroradiometric data. Inverse shutter speed was used to generate a relative skylight intensity value. Images for three time points are shown (a, b, c), along with their spectral irradiance, highlighting the spectral change as solar influence yields to lunar influence. Note the distinct aurora signature at time point b.

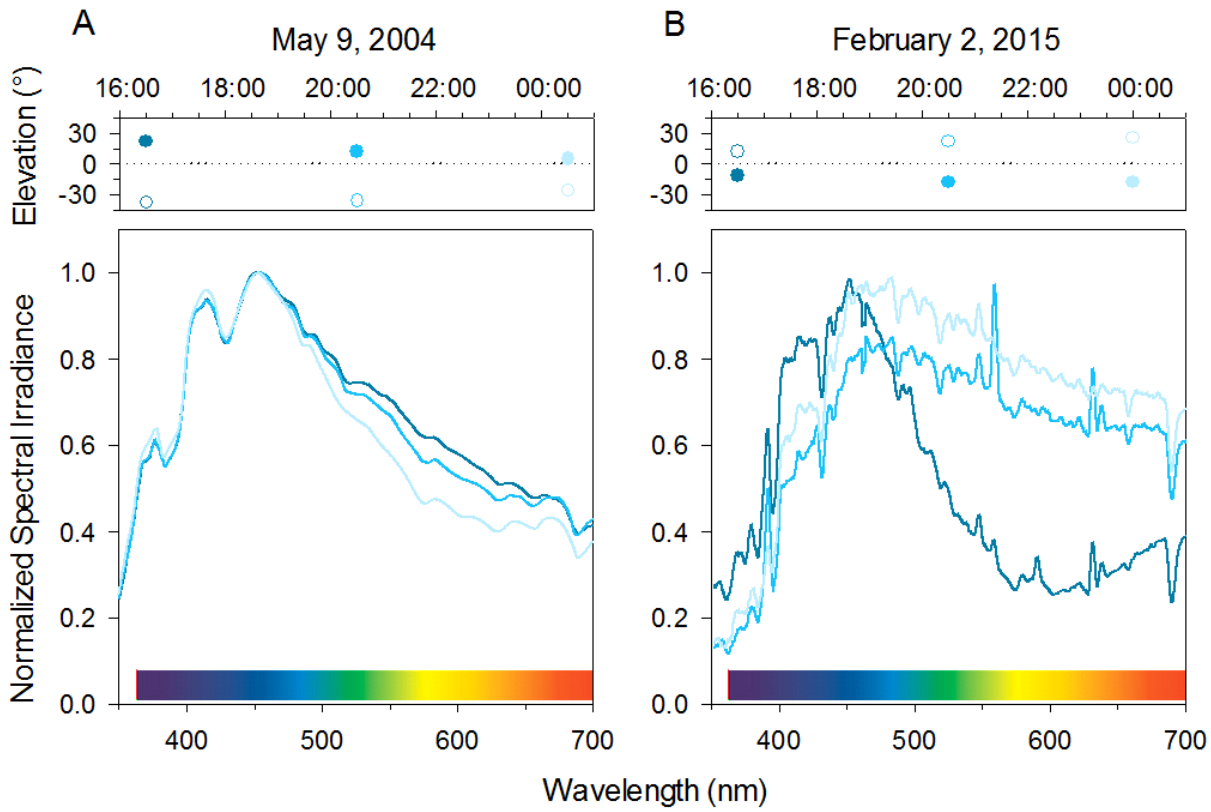

Fig 3.7 Changes in spectral irradiance when the sun or moon near the horizon. Data are irradiance ($E_{d\lambda}$) at sea level in Ny-Ålesund. (**a**, upper and lower panels) Midnight sun in May, when the sun (filled circles, upper panel) is always above the horizon and the moon (open circles circles) is always below the horizon. The sun contributes most to $E_{d\lambda}$ at this time. (**b**, upper and lower panels) Polar Night in February, when the moon is always above the horizon and the sun is always below the horizon. The moon contributes most to $E_{d\lambda}$ at this time. Colors associated with the visible spectrum are provided with each panel. For both midnight sun and Polar Night, the spectra are reduced at yellow wavelengths during the times when the dominant light source (sun during midnight sun, or moon during Polar Night) is near the horizon, and accordingly the path length for its light is the longest at that point of the diel cycle

3.4 Underwater light in the Polar Night

The underwater light climate is dependent upon (1) atmospheric light sources, such as the sun and moon, (2) any in-water light sources, primarily bioluminescence, and (3) the optical properties of the water that influence propagation of these light sources. We have already described atmospheric light during Polar Night (section 3.3), and focus here on the latter two aspects.

3.4.1 Propagation of atmospheric light through the water column

Measuring the underwater light field during Polar Night is challenging due to the detection limits of commercially available light sensors. This will no doubt change as sensor technology develops. For now, our understanding of underwater light during the Polar Night comes primarily from radiative transfer models incorporating observations of atmospheric light (i.e., diffuse sky irradiation) and the inherent optical properties (IOPs) of fjordic waters in Svalbard. These models yield predictions of the underwater spectral irradiance during Polar Night (Fig. 3.8). Overall, this work suggests the optically clear water present during Polar Night is similar to that of early spring, prior to the spring bloom and extensive freshwater runoff. Downwelling irradiance ($E_{d\lambda}$) in the water column has a spectral transmission maximum in the blue spectral region, with a broad peak at ~455 nm in shallow waters transitioning to a narrower peak at ~495 nm by 100 m depth.

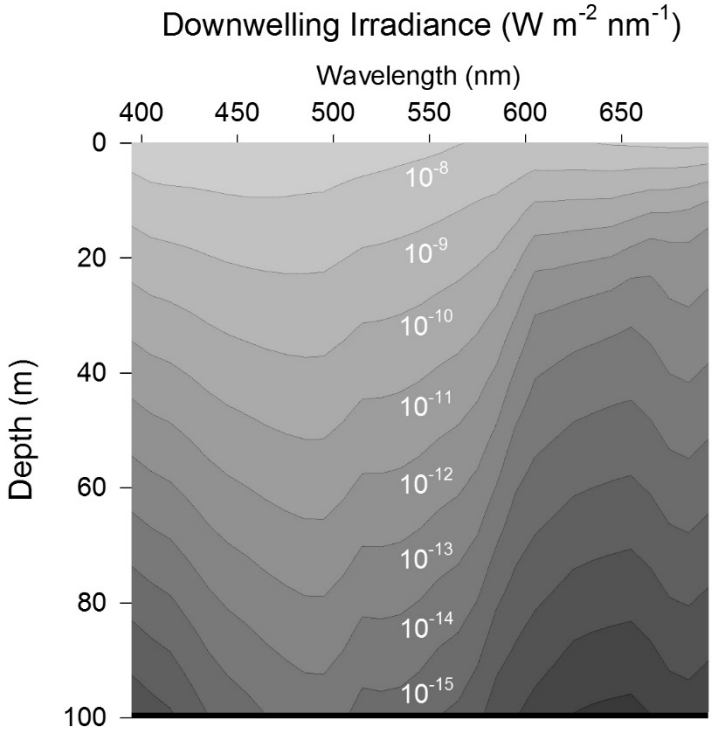

Fig 3.8 Modelled underwater spectral light field in Kongsfjorden at midday under clear sky conditions. Contours show the ambient underwater light as downwelling spectral irradiance ($E_{d\lambda}$, µmol photons m^{-2} s^{-1} nm^{-1}) derived from the radiative transfer model HydroLight. Data were replotted from Cronin et al. (2016)

The bulk optical properties of seawater determine what happens to photons as they travel through the water column, and in turn generate the spectral attenuation described above. Photons can be absorbed or scattered by water molecules and the particulate and/or dissolved constituents in water, and it is these absorption and scattering properties that are termed Inherent Optical Properties, or IOPs (Johnsen et al. 2009). IOPs are independent of the ambient light field and will not change with changes in incident light, as compared to apparent optical properties, described below, which are dependent on solar intensity, angle, etc. IOPs are commonly described in terms of light absorption, $a(\lambda)$ and scattering, $b(\lambda)$ coefficients. Light beam attenuation, $c(\lambda)$ is therefore defined by $a(\lambda) + b(\lambda)$. As particulate and dissolved substances in a parcel of seawater change with time and/or depth, so will its IOPs. For example, fjord and coastal waters of Svalbard vary seasonally in terms of phytoplankton (using [chl a] as a measure of biomass), coloured dissolved organic matter (cDOM), and total suspended matter (TSM) (Johnsen et al. 2009, Leu et al. 2011, Hovland et al. 2014, Hancke et al. 2014) which will each increase IOPs and light attenuation. Interestingly, little cDOM is locally produced as top soil is limited on Svalbard (Johnsen et al. 2009; see Chapter 4), leaving primary production and suspended material as primary factors affecting IOPs in this region.

While *in situ* observations of IOPs are available for a range of Arctic locations, these tend to focus on spring and summer periods. This timing reflects a goal of understanding biological impacts of optical conditions with seasonal sea ice cover and melt, the spring bloom, and suspended sediment from glacial freshwater runoff (e.g., Pegau 2002, Granskog et al. 2015, Hancke et al. 2014, Hovland et al. 2014, Pavlov et al. 2015, 2016, Sagan and Darecki 2018). Comparable IOP measurements during Polar Night are limited to Kongsfjorden, Svalbard (Cohen et al. 2015). These data suggest low IOP values that are homogeneous with depth below the upper ~10 m, reflecting a well-mixed water column. For comparison, Sagan and Darecki (2018) measured IOPs for specific water masses in Kongsfjorden (e.g., Cottier et al. 2005; see Chapter 2) during late July post-bloom conditions with high runoff in surface water. Polar Night IOPs align with Atlantic Water from this study. Atlantic Water in Kongsfjorden has lower overall absorption, scattering, and attenuation than other water masses in the fjord (Fig 3.9A,B); these other water masses are more influenced by local biological production, cDOM and TSM from freshwater runoff. Consistent with this, Polar Night IOPs are comparable to those measured by Pavlov et al. (2015) prior to the spring bloom in Atlantic Water of the West Spitsbergen Current off Kongsfjorden.

Another common way to quantify the underwater light field is through the Apparent Optical Properties of seawater, or AOPs, which depend on both IOPs and the ambient radiance distribution. AOPs include the diffuse attenuation coefficients for radiance and irradiance (e.g., K_d PAR). Because AOPs vary with both IOPs and the ambient light field, they are altered and regulated by factors such as: sun angle (affecting light intensity and spectral composition), albedo, surface waves, dynamic changes in cloud cover, rain, snow and air humidity (Sakshaug et al. 2009). Regardless, AOPs are relatively straightforward to measure and provide a valuable metric for describing the underwater light field, and light attenuation through snow/ice/water (e.g., Light et al. 2015). Hanelt et al. (2001) reported K_d PAR in Kongsfjorden from May through September, encapsulating the spring bloom (Fig. 3.9C). The lowest diffuse attenuation coefficients from that study correspond to those determined from radiative transfer models for underwater light during

Polar Night (K_d PAR = 0.18 m^{-1}; Cronin et al. 2016). These values are also comparable to AOPs measured in Kongsfjorden during pre-bloom spring conditions in May 2004 (Volent et al. 2007).

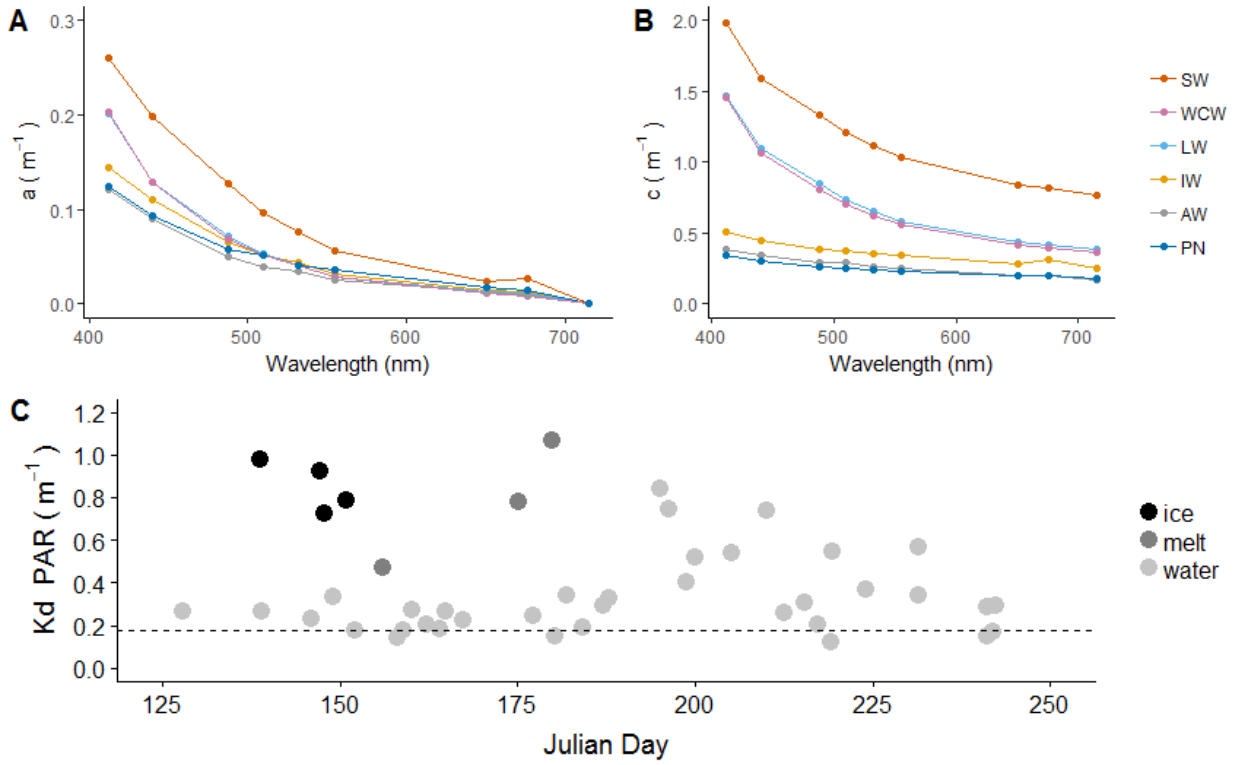

Fig 3.9 Optical properties of Kongsfjorden during Polar Night compared to other times of year. (A, B) Inherent Optical Properties (IOPs) measured during Polar Night (Cohen et al. 2015) and summer (Sagan and Darecki 2018). Panel shows absorption ($a(\lambda)$) and panel B shows beam attenuation ($c(\lambda)$) for Polar Night (PN), along with summer measurements for Surface Water (SW), Winter Cooled Water (WCW), Local Water (LW), Intermediate Water (IW), Atlantic Water (AW). (C) Apparent Optical Properties (AOPs) represented by $K_{d,PAR}$ plotted as a function of Julian Day, replotted from Hanelt et al. (2001). $K_{d,PAR}$ was calculated from vertical radiometric profiles in 1995-1998, including: four from rare "ice" periods when sea ice was present in the fjord in early spring (black circles); three from "melt" periods when turbid melt water influenced the upper water column (dark grey circles); and the remainder (n=36) from "water" periods with open water. Dashed line represents $K_{d,PAR}$ for Polar Night calculated from a modelled light field (Cronin et al. 2016)

3.5 Bioluminescence contributes to the underwater light field

3.5.1 Bioluminescence as a phenomenon

In addition to atmospheric ambient light sources, biologically produced light represents another source of photons to the underwater light environment during Polar Night. Bioluminescence is a ubiquitous phenomenon in the world's oceans and plays significant roles in animal behavior. Bioluminescence is used in marine organisms for an array of specific defensive purposes using the light generated to startle, avoid, misdirect, and camouflage (see Chapter 11, Fig. 11.18). Offensive uses of bioluminescence include luring prey, stunning prey with light, and illuminating potential

prey. Finally, bioluminescence functions in intra-species communication for mate attraction/recognition. Haddock et al. (2010) fully summarized and reviewed these behavioral adaptations and the diversity of luminous taxa. Given the prevalence of bioluminescence it is also not surprising that the spectral peak of bioluminescence (470- 490 nm; Widder 2010) is near the maximum transmission wavelength in clear ocean water (e.g., Fig. 3.8), as well as the highest sensitivity for vision in many fish and zooplankton (Turner et al. 2009, Warrant and Lockett 2004).

For the behavioral adaptations listed above to be effective, one would assume bioluminescence intensity must be higher than the ambient background light. These conditions would exist during periods and locations controlled by the periodicity of atmospheric light and a dynamic depth where functional light (for vision/detection) transitions exponentially to darkness. In addition to direct differences between intensities of bioluminescent and ambient light, there are endogenous rhythms of bioluminescent potential in organisms, which modulate bioluminescence intensity and is often synchronous with the ambient light environment (Batchelder et al. 1992). These conditions restrict the study of bioluminescence in the field to night hours and to the deep sea, an environment inherently difficult to study.

3.5.2 Bioluminescent taxa during Polar Night

Spectral irradiance during Polar Night is comparable to light at mesopelagic depths (e.g., Kaartvedt et al. 2019), where prolonged low solar/lunar irradiance results in the depth of transition to "darkness" in the water column occurring in shallow water (<50 m) (Fig. 3.10). Until recently, however, only a few studies had quantified bioluminescent organisms and the bioluminescence potential (potential maximum light intensity per organism) in Polar regions, and none during Polar Night. Buskey (1992) examined bioluminescence distributions and community structure during the spring in the Greenland Sea off Svalbard with the goal of developing methodology to use bioluminescence as a way to measure total biomass and light budgets of a given water mass. The majority of epipelagic bioluminescence was correlated with zooplankton. Specifically, it was produced by copepods (*Metridia* spp.), larvaceans (*Oikopleura* spp.), euphausiids (*Thysanoeassa* spp.) and ostracods (*Conchoecia* spp.). The contribution of bioluminescent organisms was found to vary significantly over that two-month study (Buskey 1992). Bioluminescent dinoflagellates (*Protoperidinium* spp.) were rare and did not contribute significantly to bioluminescence. Lapota et al. (1989, 1992) conducted studies in the Beaufort Sea during the autumn and in summer in Vestfjorden, northern Norway, respectively. In those studies, *Protoperidinium* spp. was abundant and accounted for between 20 and 90% of the total light budget in the upper 100 m in the Beaufort Sea and up to 96% of the total light budget in Vestfjorden, respectively. Vestfjorden had zooplankton assemblages similar to those in the Greenland Sea (*Metridia longa, M. lucens*, *Conchoecia* spp., and the euphausiid *Thysanoessa* spp.). In the Beaufort Sea, *M. longa* produced 80% of the bioluminescence potential, with *Protoperidinium* spp. producing the remaining 20%. Work on bioluminescence is even scarcer in the Southern Ocean, with one study associating bioluminescence with new species, many benthic (Raymond and DeVries 1976), and looking at the contribution of bioluminescence to elephant seal foraging (Vacquié-Garcia et al. 2012).

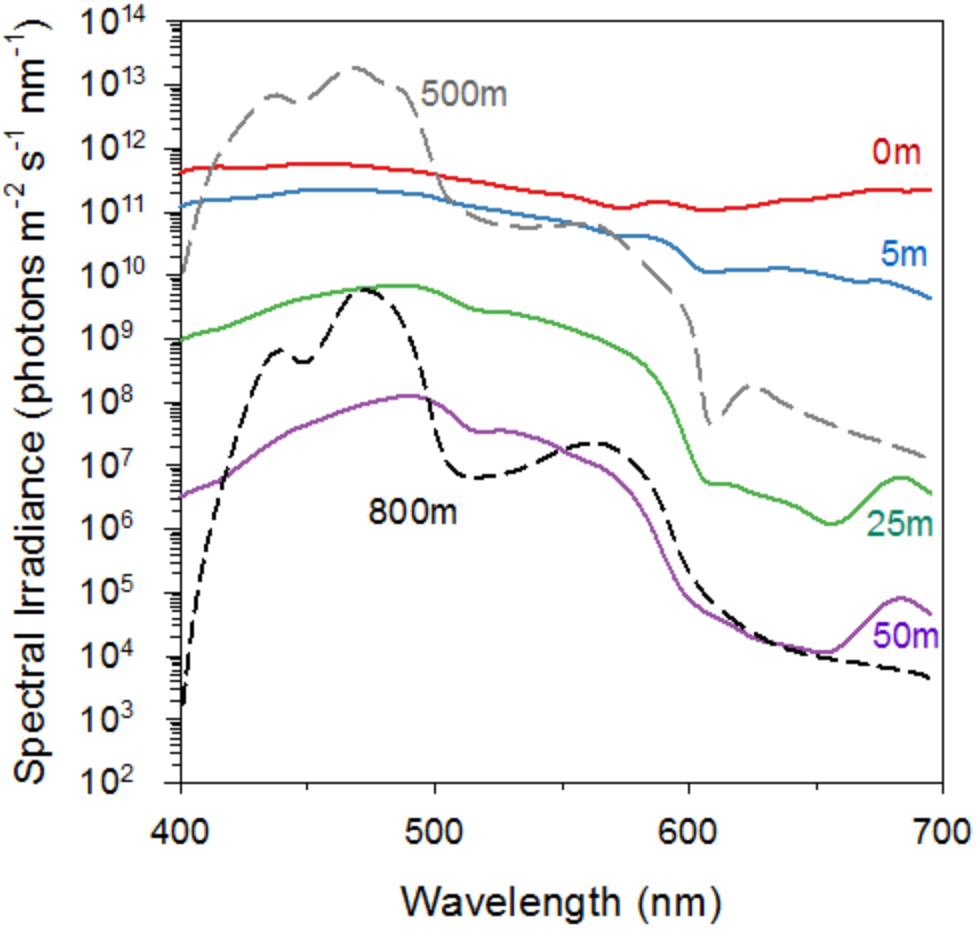

Fig 3.10 Comparison of Polar Night and deep-sea light. Data are modelled spectral irradiance for Kongsfjorden (solide lines) and the mesopelagic (dashed lines), replotted from Cronin et al. (2016) and Li et al. (2014), respectively. Both maximally transmit blue-green light, and spectral irradiance is similar between the upper 50m of Kongsfjorden and the mesopelagic.

With a general paucity of bioluminescent measurements made in high latitude regions during Polar Night, there has been a concerted effort over the last decade to expand our understanding of bioluminescent organisms, starting with an accounting of taxonomic representation. In mid-January, Berge et al. (2012) found the distribution of bioluminescent organism to be similar to previous studies (Buskey 1992, Lapota et al. 1989, 1992) with the addition of moderate numbers of *Oncaea borealis*, *Heterorhabdus noregicus*, and *Appendicularia*. While 180 μm depth-stratified nets were used in this study, an autonomous underwater vehicle (AUV) equipped with a bioluminescence bathyphotometer with 20 μm nets in the exhaust ports (Moline et al. 2004) was also employed in the same field to better understand the distributions and flash intensities of organisms. The nets on the AUV were able to capture both non-bioluminescent and bioluminescent zooplankton in Kongsfjorden in January equivalent to those caught by traditional net sampling (Berge et al. 2012). Because of the decreased mesh size, the AUV nets were also able to collect phytoplankton and showed that dinoflagellates comprised over 90% of the phytoplankton numbers

and half were luminescent *Protoperidinium* spp. The most important result in Berge et al. (2012) was the distribution of bioluminescent organisms obtained by the targeted AUV sampling. Sampling around noon and near midnight, the distribution of bioluminescence at three depths showed significant differences with higher intensities at the shallow depth at “night” and higher intensities at the deeper depth around solar noon. Bioluminescent organisms were in low abundance, spatially distributed and varied four orders of magnitude in intensity.

Like previous studies that examined only the light intensities generated from bioluminescent organisms, Johnsen et al. (2014) followed this study up by examining the flash kinetics of individual flashes, which are known to be unique to each taxa (Nealson et al. 1986) (Fig. 3.11). By collection, measurement and parameterization of the dominant luminescent organisms (*Protoperidinium* spp., *M. longa*, *Mertensia ovum*, *Beröe cucumis*, and *Meganyctiphanes norvegica*), over 80% of the bioluminescent flashes were taxonomically identified (Johnsen et al. 2014). This is a powerful tool in that bioluminescent taxa can now be mapped on the time and space information collected by the bathyphotometers (both profiling, and on AUVs). This approach was demonstrated by Cronin et al. (2016) for the upper 120 m of the water column off Svalbard. The bioluminescent community were in this study were similarly represented by *Protoperidinium* spp., *Beröe cucumis*, *Mertensia ovum*, *Metridia* spp., *Meganyctiphanes norvegica*, *Thysanoessa inermis*, and *Boroecia* spp. These data show the species depth separation and highlight the limitations of net sampling to reveal depth distributions, which is critical when evaluating vertical migration (Chapter 5) and rhythmicity (Chapter 8) of bioluminescence in the Polar Night.

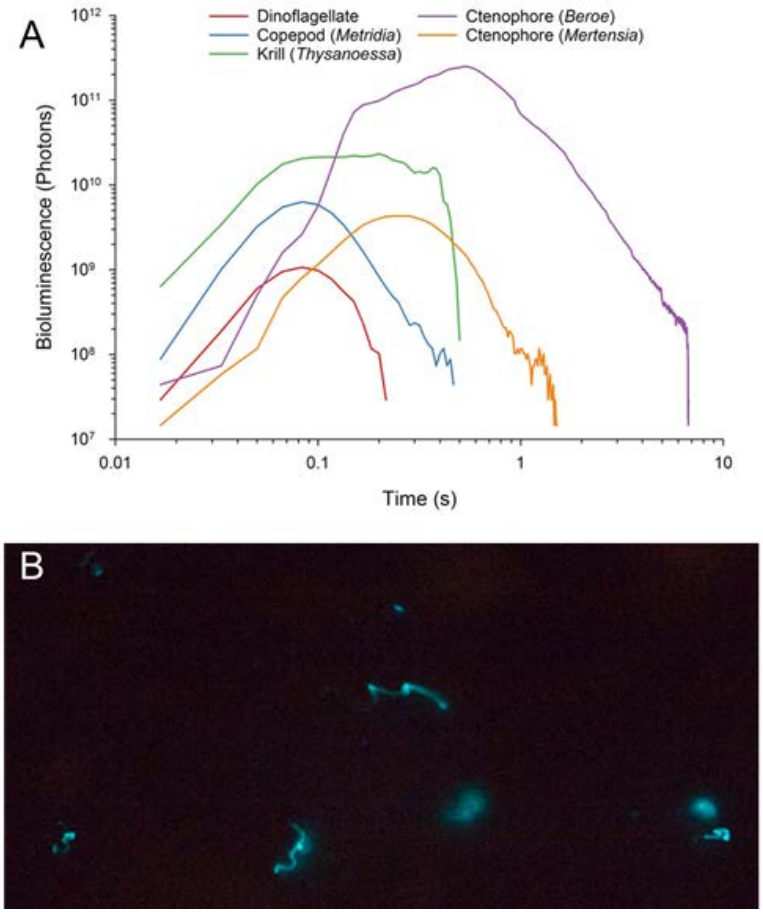

Fig 3.11 Bioluminescence of Arctic plankton common during Polar Night. (**a**) Luminescent emissions of each taxa as recorded by an *in situ* bathyphotometer (Underwater Bioluminescence Assessment Tool; UBAT) are distinguishable from one another. (**b**) A photograph taken from the Ny-Ålesund pier looking down into the water during Polar Night. Most likely, bioluminescent trails are the copepod *Metridia*, while more diffuse luminescence are from ctenophores. Photo: Geir Johnsen.

3.5.3 Rhythms in bioluminesence during Polar Night

Rhythmicity in bioluminescence has primary been examined in phytoplankton communities, with photoinhibition being the identified mechanism for measured decreases during midday (Kelly and Katona 1966, Batchelder et al. 1992). Whether this holds in zooplankton and during transition to Polar Night was the subject of recent studies. Berge et al. (2012) demonstrated that the bioluminescent community did not show variation over the day at the surface during the polar night. Similarly, Johnsen et al. (2014) showed there were no significant changes in flash intensities from individual taxa (including dinoflagellates) over a three-day period in mid-January from a fixed station continuously pumping at 20 m. Unlike these two short-term studies conducted in the middle of the Polar Night, longer-term bioluminescent data were collected from surface waters continuously over the transition period into Polar Night from September to December. Importantly, this study was conducted at the surface in shallow water as to avoid changes in bioluminescence due to vertical migration, which have been shown to continue during the Polar Night (Chapters 5 and 8). Data revealed that there was a diel pattern at the beginning of the study, but that this rhythmicity was lost in mid-November, corresponding to the start of civil polar night at this location (Fig. 3.12). Results of this time series also reveal that the loss of rhythmicity not only apply to dinoflagellates but also within the zooplankton community.

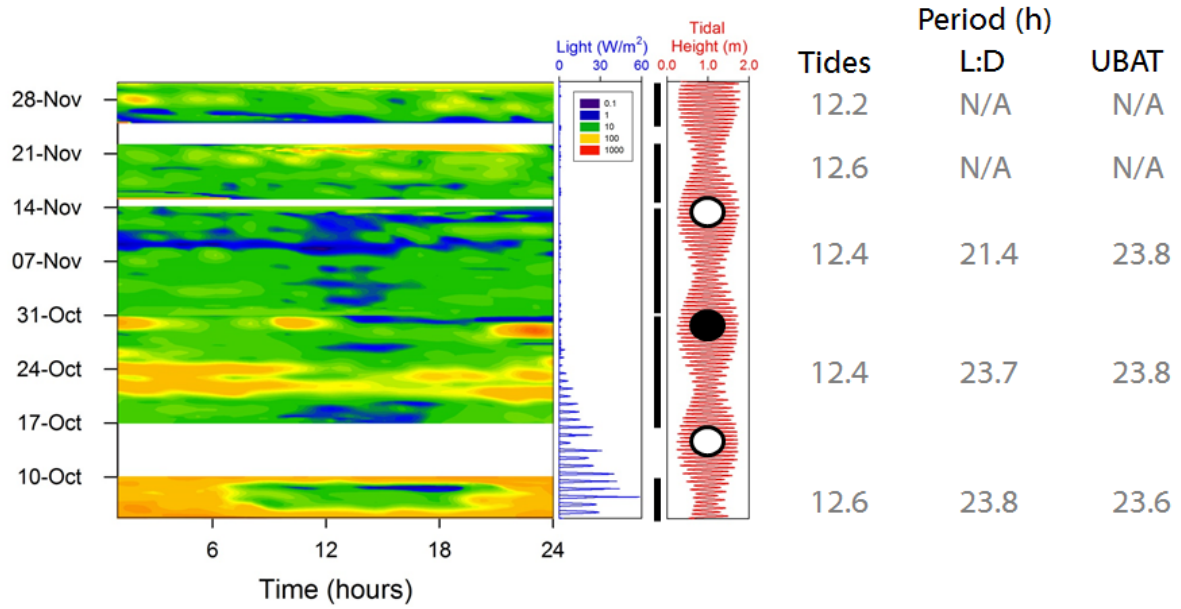

Fig 3.12 Rhythmic bioluminescence patterns decay into Polar Night. UBAT deployment at ~0.5m depth from a floating dock in Adventfjorden, Svalbard, during October - November 2011. Left panel is bioluminescence (log photons h^{-1}) with white sections indicating data gaps. Corresponding light (BSRN shortwave pyranometer, Ny-Ålesund) and tides (Longyearbyen) are plotted in right panels. Black lines indicate five separate sections for which the time series were analyzed for period with Maximum Entropy Spectral Analysis (numbers on right). While tides remain periodic throughout the time series, light decreases below detection with this sensor and becomes arrhythmic by mid-November, as does the UBAT signal

3.5.4 Spatial distribution of bioluminescence during Polar Night

In addition to these focused studies on taxonomy, flash kinetics, and rhythmicity, the larger scale distributions of bioluminescence in the Polar Night have been evaluated. In January 2012, a series

of stations were occupied along a transect from mainland Norway to 82° N north of Svalbard. Profiles of bioluminescence were measured at these stations along with standard oceanographic variables (temperature, salinity, fluorescence). For the portion of this transect stretching between Rijpfjorden to the Marginal Ice Zone (Fig 3.13A), the distribution of bioluminescence was not correlated to any of these variables or derived variables of the physical structure of the water column (density, buoyancy frequency). Taken together, there was an inverse relationship between bioluminescence and depth (Fig. 3.13B), similar to findings of Buskey (1992) during spring in the same region. While profiles taken along a transect are able to capture the broad scale distributions, interpretation is problematic as they do not capture the time-dependent variability of vertical migration and response to the day length which are known to influence the vertical distribution of organisms as well as bioluminescence intensity by 2-3 orders of magnitude. Ideally, daily stations would be occupied along a latitudinal gradient to elucidate the response and importance of organismal bioluminescence in the water column to the gradient in atmospheric light when approaching the pole.

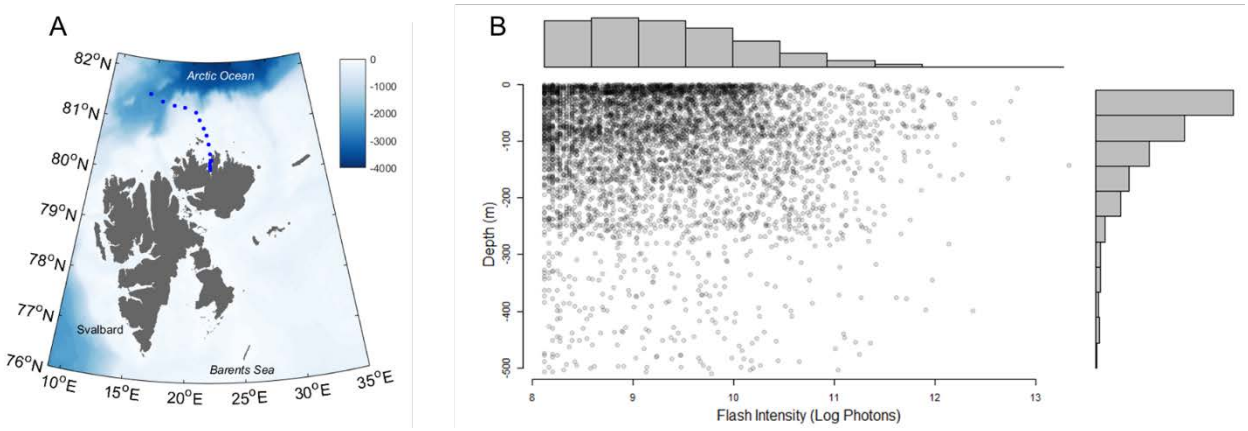

Fig 3.13 Bioluminescence transect from Rijpfjorden (Svalbard) into the Marginal Ice Zone during January 2012. (A) Stations (blue circles) where bioluminescence profiles were conducted. (B) Intensity (log photons) of each bioluminescence flash captured during these profiles. Histograms show the distributions of flash intensity (x-axis) and depth (y-axis). Median bottom depth among these stations was 273m

3.5.4 Bioluminescence and predator-prey interactions during Polar Night

The complexity and roles that bioluminescence plays in predator-prey interactions has been a challenging topic to understand. Visual cues for predators and prey alike are a combination of available light, which originates either from the atmosphere (see 3.4.1) or internally within the water column through bioluminescence, and the visual sensitivities of the organisms involved (Box 3.1). Cronin et al. (2016) mapped the vertical photon budget and the depth of transition from atmospheric light to that dominated by bioluminescence (Fig. 3.13). Over a relatively small depth range of 20 m, bioluminescent light transitioned from contributing less than 3% of the pelagic photon budget to over 85%, and below 60 m bioluminescence contributed over 98% of the pelagic photon budget. Interestingly, Cronin et al. (2016) also documented a change in the bioluminescent

community in that depth range which is suggestive that this transition may play a functional role of bioluminescence in predator-prey interactions.

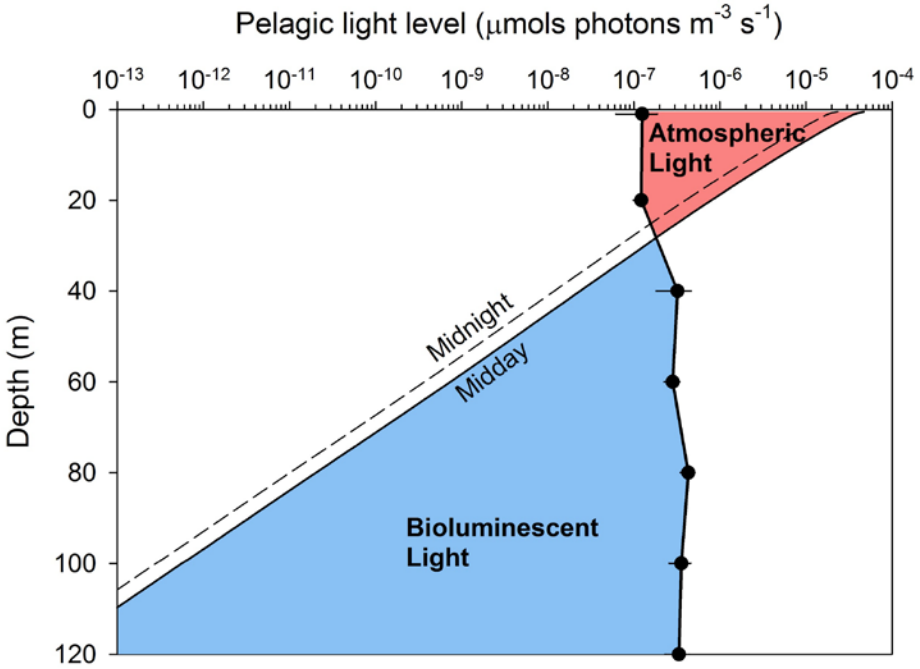

Fig 3.13 Photon budget for biological and atmospheric light sources in Kongsfjorden during Polar Night. The two components of the underwater light field in Kongsfjorden are plotted as a function of depth in equivalent volumetric units (μmol photons m^{-3} s^{-1}). Atmospheric light is scalar irradiance (solid line; 400-700 nm, $E_{o,PAR}$) modeled from diffuse atmospheric irradiance measured at midday (solid line) and midnight (dashed line) in January. Bioluminescence is mean bioluminescence potential (± SE, black dots). The colors represent photic zones dominated by atmospheric light (red shading) and bioluminescent light (blue shading). Data are replotted from Cronin et al. (2016)

3.6 Artificial light in Polar Night

As detailed above and in subsequent chapters (e.g., Chapters 4-8), low levels of ambient illumination are important for regulating biological processes during Polar Night. However, in "dark" habitats such as this, with organisms exhibiting capabilities of detecting and responding to extreme low levels of light, additional light can become a problem. At least artificial light, which becomes *light pollution*.

The area affected by artificial illumination at night is increasing by 6% per year on average, thus becoming one of the fastest-spreading environmental challenges of the Anthropocene (Hölker et al. 2010). An estimated 23% of all land masses between 75°N and 60°S are now believed to be exposed to scattered artificial light that is reflected back to the ground from the atmosphere (Falchi et al. 2016). Few pristine dark habitats above ground remain, and artificial lights from cities, coastlines, roads and marine infrastructures are visible from outer space. The Arctic Polar Night is, arguably, one of the last undisturbed dark habitats on the planet. However, with increased human presence in the Arctic, this may be about to change.

Pollution and other anthropogenic disturbances of biological systems are widespread across the planet, with rising CO_2 levels causing global warming being one of the most important. Even in sparsely populated areas of the Arctic, footprints of human activities are noticeable (Wassmann et al. 2011). However, while changing temperature, pH, ice cover, and CO_2 levels are all factors that naturally have affected biological communities throughout evolutionary history, anthropogenic light pollution is an unprecedented phenomenon starting by the end of 1800 century. Hence, while some taxa have adaptations that have evolved in relation to, for example, changing pH levels (Kelly et al. 2013) or ice cover (Berge et al. 2012), none have had the opportunity to evolve in relation to light pollution. Rather, the harmonic movements of the earth, moon and sun provide reliable cues to which many biological events are now highly attuned (Chapter 8). For polar regions, the intensities of these cues have, arguably, changed with changing ice cover over time, but not the periodicity and harmonic cyclic events. Although light pollution is globally widespread and expanding, we know very little about its potential effects at high latitudes. Arguably, the lack of attention towards light pollution in the Arctic is due to two factors: First, the Arctic is still sparsely populated, with vast regions unaffected by human settlements. Second, as described above, the light climate that governs polar regions is unique and extreme, with most of the biological activity assumed to occur outside of the darkest portions of the year (see Chapter 1 for historical discussion). Ambient darkness can be defined both in space (e.g., deep sea, polar versus temperate regions) and in time (night versus day). The Arctic polar night is a combination of both. However, while the deep sea is likely to remain largely unaffected by light pollution, the Arctic Polar Night is seeing an increase in human activity (Chapter 10) – and hence light pollution.

While not well-studied, light pollution in polar habitats at night, and during Polar Night, has been documented. Euphausiids (krill) on the Nova Scotia continental shelf during nighttime avoid artificial light from ships (Sameoto et al. 1985). Furthermore, artificial light is known to affect the distribution of fish, either by attracting or repulsing them (Marchesan et al. 2005, Nightingale et al. 2006). In work done during Polar Night, Ludvigsen et al. (2018) demonstrated that quick and consistent avoidance responses occur for the entire zooplankton and pelagic fish community

when presented with artificial light from research vessels. These data show how even reduced and indirect artificial light from a ship biases measurements of abundance, distribution and behaviour of both zooplankton and fish. The potential implication of this study related to stock assessments and acoustic surveys carried out not only in the Arctic, but also in the dark more generally, are significant. Norwegian vessels conduct sampling "24/7" during stock assessment cruises, not considering if the acoustics or trawl hauls are carried out at day or night. A comparable review from Fisheries and Oceans Canada indicate that at least 25% of all assessments using bioacoustics are carried out at night.

3.7 Future perspectives and knowledge gaps

While observations and modeling of light during Polar Night are growing, numerous gaps remain. We review several key ones here.

1. Observational capacity. Conventional radiative transfer models are limited at low solar elevations, making observations essential. Existing data on light during Polar Night is limited to a few locations (e.g., Svalbard). Numerous factors contribute to this, including instrumentation available for low-level spectroradiometric measurements, and infrastructure for sustained observations throughout polar night. Camera-based measurements (e.g., Zolich 2018, Jechow et al. 2019) hold promise, and commercially available fiber-optic spectroradiometers are increasingly more sensitive (Johnsen 2012), addressing the former issue. Regarding infrastructure, a combination of fixed observatories (e.g., *ArcLight*) and autonomous platforms (Chapter 9) will both be essential to make sustained light measurements over the course of the year at high latitudes.
2. Environmental change. Polar environments are changing – atmospheric conditions and precipitation, the quantity and quality of Arctic sea ice, extent and influence of glacial meltwater, and location of marine water masses. All of these examples have the potential to alter the Arctic light environment during Polar Night, either through direct changes in the spectral irradiance entering the water, or indirect changes in IOPs which then influence the underwater light field. Changes to the underwater light field will affect primary productivity (Chapter 4) and predator/prey dynamics (Langbehn and Varpe 2017, Varpe et al. 2018).
3. Light pollution. Recent decades have seen increasing levels of light pollution globally, changing the intensity, spectral composition and photoperiod of night light. This makes it difficult to quantify "natural" light during Polar Night, even at remote locations (e.g., Jechow et al. 2019). We currently lack an understanding of the artificial light signal during polar night, and what effect it has on biology. However, we do know that light pollution can impact behavior of pelagic marine life during Polar Night (Ludvigsen et al. 2018). Beyond ecological effects of artificial light, the potential for vessel light pollution related to stock assessments and acoustic surveys carried out not only in the Arctic, but also in the dark in general, are immense.
4. Photoperiod. While the duration of day and night seems like a simple concept, it is complex when considering that for biological systems the spectral composition of the light field and the spectral responsivity of the light detector must be aligned. This applies to both marine

and terrestrial organisms. It is further complicated by the changing spectral conditions over the course of the year, most notably during polar night. To quantify "photoperiod" for a given organism we need to understand both the light environment at the location and perspective of the organism, as well as its ability to detect both the wavelength and intensity. Given the role photoperiod plays in biology during Polar Night (Chapters 4-8), quantifying this aspect of light is a priority.

References

Albini A (2016) Some remarks on the first law of photochemistry. Photochem Photobiol Sci 15:319-324. https://doi.org/10.1039/C5PP00445D

Anthony PD, Hawkins AD (1983) Spectral sensitivity of the cod, *Gadus morhua* L. Mar Behav Physiol 10:145-166. http://dx.doi.org/10.1080/10236248309378614

Batchelder H, Swift E, Van Keuren J (1992) Diel patterns of planktonic bioluminescence in the northern Sargasso Sea. Mar Biol 113:329-339 (1992). https://doi.org/10.1007/BF00347288

Båtnes AS, Miljeteig C, Berge J, Greenacre M, Johnsen G (2015) Quantifying the light sensitivity of Calanus spp. during the polar night: potential for orchestrated migrations conducted by ambient light from the sun, moon, or aurora borealis? Polar Biol 38:51-65. http://dx.doi.org/10.1007/s00300-013-1415-4

Berge J, Båtnes AS, Johnsen G, Blackwell SM, Moline MA (2012) Bioluminescence in the high Arctic during the polar night. Mar Biol 159:231–237. https://doi.org/10.1007/s00227-011-1798-0

Berge J, Daase M, Renaud PE, Ambrose, Jr WG, Darnis G, Last KS, Leu E, Cohen JH, Johnsen G, Moline MA, Cottier F, Varpe Ø, Shunatova N, Balazy P, Morata N, Massabuau JC, Falk-Petersen S, Kosobokova K, Hoppe CJM, Węsławski JM, Kuklinski P, Legeżyńska J, Nikishina D, Cusa M, Kędra M, Włodarska-Kowalczuk M, Vogedes D, Camus L, Tran D, Michaud E, Gabrielsen TM, Granovitch A, Gonchar A, Krapp R, Callesen TA (2015) Unexpected levels of biological activity during the polar night offer new perspectives on a warming Arctic. Current Biol 25:1-7. http://dx.doi.org/10.1016/j.cub.2015.08.024

Bond DS, Henderson FP (1963) The conquest of darkness. AD 346297. Defense Documentation Center. Alexandria, VA.

Buskey EJ (1992) Epipelagic planktonic bioluminescence in the marginal ice-zone of the Greenland Sea. Mar Biol 113:689-698. https://doi.org/10.1007/BF00349712

Cohen JH, Berge J, Moline MA, Sørensen AJ, Last K, Falk-Petersen S, Renaud PE, Leu ES, Grenvald J, Cottier F, Cronin H, Menze S, Norgren P, Varpe Ø, Daase M, Darnis G, Johnsen G (2015) Is Ambient Light during the High Arctic Polar Night Sufficient to Act as a Visual Cue for Zooplankton? PLoS ONE 10(6): e0126247. http://dx.doi.org/10.1371/journal.pone.0126247

Cottier F, Tverberg V, Inall M, Svendsen H, Nilsen F, Griffiths C (2005) Water mass modification in an Arctic fjord through cross-shelf exchange: The seasonal hydrography of Kongsfjorden, Svalbard. J Geophys Res 110: C12005. https://doi.org/10.1029/2004JC002757

Cronin, T, Johnsen S, Marshall NJ, Warrant EJ (2014) Visual Ecology. Princeton University Press. ISBN 9780691151847

Cronin HA, Cohen JH, Berge J, Johnsen G, Moline MA (2016) Bioluminescence as an ecological factor during high Arctic polar night. Sci Rep 6:36374. http://dx.doi.org/10.1038/srep36374

Granskog MA, Pavlov AK, Sagan S, Kowalczuk P, Raczkowska A, Stedmon CA (2015) Effect of sea-ice melt on inherent optical properties and vertical distribution of solar radiant heating in Arctic surface waters. J Geophys Res Oceans 120:7028-7039. https://doi.org/10.1002/2015JC011087

Haddock SH, Moline MA, Case JF (2010) Bioluminescence in the sea. Ann Rev Mar Sci 2:443-493. https://doi.org/10.1146/annurev-marine-120308-081028

Hancke K, Hovland EK, Volent Z, Pettersen R, Johnsen G, Moline MA, Sakshaug E (2014) Optical properties of CDOM across the Polar Front in the Barents Sea: Origin, distribution and significance. J Mar Syst 130: 219-227. http://dx.doi.org/10.1016/j.jmarsys.2012.06.006

Hancke K, Lund-Hansen LC, Lamare ML, Pedersen SH, King MD, Andersen P, Sorrell BK (2018) Extreme low light requirement for algae growth underneath sea ice: a case study from Station Nord, NE Greenland. J Geophys Res Oceans 123:985-1000. http://dx.doi.org/10.1002/2017JC013263

Hanelt D, Tüg H, Bischof K, Groß C, Lippert H, Sawall T, Wiencke C (2001) Light regime in an Arctic fjord: a study related to stratospheric ozone depletion as a basis for determination of UV effects on algal growth. Mar Biol 138:649-658. https://doi.org/10.1007/s002270000481

Hisdal V (1986) Spectral distribution of global and diffuse solar radiation in Ny-Alesund, Spits bergen. Polar Res 5(n .s.):1-27. https://doi.org/10.3402/polar.v5i1.6865

Hovland EK, Hancke K, Alver MO, Drinkwater K, Høkerdal J, Johnsen G, Moline MA, Sakshaug E (2014) Optical impact of an *Emiliania huxleyi* bloom in the frontal region of the Barents Sea. J Mar Syst 130:228-240. https://doi.org/10.1016/j.jmarsys.2012.07.002

Jechow A, Kyba CCM, Hölker F (2019) Beyond All-Sky: Assessing Ecological Light Pollution Using Multi-Spectral Full-Sphere Fisheye Lens Imaging. J Imaging 5:46. https://doi.org/10.3390/jimaging5040046

Johnsen G, Candeloro M, Berge J, Moline MA (2014) Glowing in the dark: discriminating patterns of bioluminescence from different taxa during the Arctic polar night. Polar Biol 37:707-713. https://doi.org/10.1007/s00300-014-1471-4

Johnsen G, Volent Z, Sakshaug E, Sigernes F, Pettersson LH (2009) Remote sensing in the Barents Sea. Pp 139–166. In Sakshaug E, Johnsen G, Kovacs K. (eds). Ecosystem Barents Sea. Tapir Academic Press, Trondheim. ISBN 978-82-519-2461-0

Johnsen S (2012) The Optics of Life. Princeton University Press. ISBN 9780691139913

Kaartvedt S, Langbehn TJ, Aksnes D.L. (2019) Enlightening the ocean's twilight zone, ICES J Mar Sci fsz010. https://doi.org/10.1093/icesjms/fsz010

Kelly MG, Katona S (1966) An endogenous diurnal rhythm of bioluminescence in a natural population of dinoflagellates. Biol Bull 131:115-126. https://doi.org/10.2307/1539652

Land MF, Nilsson D-E (2012) Animal Eyes, 2nd ed. Oxford University Press, Oxford. ISBN 978-0-19-958114-6

Langbehn TJ, Varpe Ø (2017) Sea-ice loss boosts visual search: fish foraging and changing pelagic interactions in polar oceans. Global Change Biol 23:5318–5330. https://doi.org/10.1111/gcb.13797

Lapota D, Geiger ML, Stiffey AV, Rosenberger DE, Young DK (1989) Correlations of planktonic bioluminescence with other oceanographic parameters from a Norwegian fjord. Mar Ecol Prog Ser 55:217-227. https://doi.org/10.3354/meps055217

Lapota D, Rosenberger DE, Liebermann SH (1992) Planktonic bioluminescence in the pack ice and the marginal ice zone of the Beaufort Sea. Mar Biol 112:665-675. https://doi.org/10.1007/BF00346185

Last KS, Hobbs L, Berge J, Brierley AS, Cottier F (2016) Moonlight drives ocean-scale mass vertical migration of zooplankton during the Arctic winter. Current Biol 26:244-251. https://doi.org/10.1016/j.cub.2015.11.038

Leu E, Søreide JE, Hessen DO, Falk-Petersen S, Berge J (2011) Consequences of changing sea-ice cover for primary and secondary producers in the European Arctic shelf seas: Timing, quantity, and quality. Prog Oceanogr 90:18-32. https://doi.org/10.1016/j.pocean.2011.02.004

Li L, Stramski D, Reynolds R (2014) Characterization of the solar lightfield within the ocean mesopelagiczone based on radiative transfer simulations. Deep-Sea Res I 87:53-69. http://dx.doi.org/10.1016/j.dsr.2014.02.005

Light B, Perovich DK, Webster MA, Polashenski C, Dadic R (2015) Optical properties of melting first-year Arctic sea ice. J Geophys Res Oceans 120:7657–7675. https://doi.org/10.1002/2015JC011163

Ludvigsen M, Berge J, Geoffroy M, Cohen JH, De La Torre PR, Nornes SM, Singh H, Sørensen AJ, Daase M, Johnsen G (2018) Use of an autonomous surface vehicle reveals small-scale diel vertical migrations of zooplankton and susceptibility to light pollution under low solar irradiance. Sci Adv 4. https://doi.org/10.1126/sciadv.aap9887

Maturilli M, Herber A, König-Langlo G (2015) Surface radiation climatology for Ny-Ålesund, Svalbard (78.9 N), basic observations for trend detection. Theor Appl Climatol 120:331-339. https://doi.org/10.1007/s00704-014-1173-4

Moline MA, Blackwell SM, von Alt C, Allen B, Austin T, Case J, Forrester N, Goldsborough R, Purcell M, Stokey R (2005) Remote environmental monitoring units: an autonomous vehicle for characterizing coastal environments. J Atm Ocean Tech 22:1797-1808. https://doi.org/10.1175/JTECH1809.1

Myslinski TJ, Frank TM, Widder EA (2005) Correlation between photosensitivity and downwelling irradiance in mesopelagic crustaceans. Mar Biol 147:619-629. https://doi.org/10.1007/s00227-005-1606-9

Palmer G, Johnsen S (2015) Downwelling spectral irradiance during evening twilight as a function of the lunar phase. Appl Opt 54: B85-B92. https://doi.org/10.1364/AO.54.000B85

Pavlov AK, Granskog MA, Stedmon CA, Ivanov BV, Hudson SR, Falk-Petersen S (2015) Contrasting optical properties of surface waters across the Fram Strait and its potential biological implications. J Mar Syst 143:62-72. https://doi.org/10.1016/j.jmarsys.2014.11.001

Pavlov AK, Stedmon CA, Semushin AV, Martma T, Ivanov BV, Kowalczuk P, Granskog MA (2016) Linkages between the circulation and distribution of dissolved organic matter in the White Sea, Arctic Ocean. Cont Shelf Res 119:1-13. https://doi.org/10.1016/j.csr.2016.03.004

Pavlov AK, Leu E, Hanelt D, Bartsch I, Karsten U, Hudson SR, Gallet JC, Cottier F, Cohen JH, Berge J, Johnsen G, Maturilli M, Kowalczuk P, Sagan S, Meler J, Granskog MA (2019) The Underwater Light Climate in Kongsfjorden and Its Ecological Implications. In: Hop H., Wiencke C. (eds) The Ecosystem of Kongsfjorden, Svalbard. Advances in Polar Ecology, vol 2. Springer, Cham. https://doi.org/10.1007/978-3-319-46425-1_5

Pegau WS (2002) Inherent optical properties of the central Arctic surface waters. J Geophys Res 107:8035. https://doi.org/10.1029/2000JC000382

Raymond JA, DeVries AL (1976) Bioluminescence in McMurdoSound, Antarctica. Limnol Oceanogr 21:599-602. https://doi.org/10.4319/lo.1976.21.4.0599

Sakshaug E, Johnsen G, Volent Z (2009) Light. Pp 117-138. In Sakshaug E, Johnsen G, Kovacs K. (eds). Ecosystem Barents Sea. Tapir Academic Press, Trondheim. ISBN 978-82-519-2461-0

Sagan S, Darecki M (2018) Inherent optical properties and particulate matter distribution in summer season in waters of Hornsund and Kongsfjordenen, Spitsbergen. Oceanologia 60:65-75. https://doi.org/10.1016/j.oceano.2017.07.006

Rieke F, Baylor DA (1998) Single-photon detection by rod cells of the retina. Rev Mod Phys 70:1027-1036. https://doi.org/10.1103/RevModPhys.70.1027

Tran D, Sow M, Camus L, Ciret P, Berge J, Massabuau JC (2016) In the darkness of the polar night, scallops keep on a steady rhythm. Sci Rep 6: 32435. https://doi.org/10.1038/srep32435

Turner JR, White EM, Collins MA, Partridge JC, Douglas RH (2009) Vision in lanternfish (Myctophidae): adaptations for viewing bioluminescence in the deep-sea. Deep Sea Res I 56:1003-1017. https://doi.org/10.1016/j.dsr.2009.01.007

Urban S, Seidelmann P.K. (2013). Explanatory Supplement to the Astro-nomical Almanac, 3rd ed., University Science Books. ISBN 978-1-891389-85-6

Vacquié-Garcia J, Royer F, Dragon AC, Viviant M, Bailleul F, Guinet C (2012) Foraging in the darkness of the Southern Ocean: influence of bioluminescence on a deep diving predator. PLoS One 7(8):e43565. https://doi.org/10.1371/journal.pone.0043565

Valle KC, Nymark M, Aamot I, Hancke K, Winge P, Andresen K, Johnsen G, Brembu T, Bones AM (2014) System Responses to Equal Doses of Photosynthetically Usable Radiation of Blue, Green, and Red Light in the Marine Diatom *Phaeodactylum tricornutum*. PLoS ONE 9(12): e114211. https://doi.org/10.1371/journal.pone.0114211

Varpe Ø, Daase M, Kristiansen T (2015) A fish-eye view on the new Arctic lightscape, ICES J Mar Sci, 72:2532-2538. https://doi.org/10.1093/icesjms/fsv129

Volent Z, Johnsen G, Sigernes F (2007) Kelp forest mapping by use of airborne hyperspectral imager. J App Remote Sens 1:011503. https://doi.org/10.1117/1.2822611

Vollset KW, Folkvord A, Browman HI (2011) Foraging behaviour of larval cod (*Gadus morhua*) at low light intensities. Mar Biol 158:1125-1133. https://doi.org/10.1007/s00227-011-1635-5

Warrant EJ, Locket NA (2004) Vision in the deep sea. Biol Rev Camb Philos Soc 79:671-712. https://doi.org/10.1017/S1464793103006420

Webster CN, Varpe Ø, Falk-Petersen S, Berge J, Stübner E, Brierley A (2013) Moonlit swimming: vertical distributions of macrozooplankton and nekton during the polar night. Polar Biol 38:75-85. https://doi.org/10.1007/s00300-013-1422-5

Widder EA (2010) Bioluminescence in the ocean: origins of biological, chemical, and ecological diversity. Science 328:704-708. https://doi.org/10.1126/science.1174269

Zolich A (2018) System integration and communication in autonomous unmanned vehicles in marine environments. PhD thesis, NTNU, Trondheim, Norway